JOURNAL OF QUATERNARY SCIENCE (2011) **26**(1) 44–58 ISSN 0267-8179. DOI: 10.1002/jqs.1425

Changing hillslope and fluvial Holocene sediment dynamics in a Belgian loess catchment

BASTIAAN NOTEBAERT,[1]* GERT VERSTRAETEN,[1] DIMITRI VANDENBERGHE,[2] ELENA MARINOVA,[1,3] JEAN POESEN[1] and GERARD GOVERS[1]

[1]Department of Earth and Environmental Sciences, KU Leuven, Heverlee, Belgium
[2]Vakgroep geologie en bodemkunde, Universiteit Gent, Gent, Belgium
[3]Centre for Archaeological Sciences, KU Leuven, Heverlee, Belgium

Received 22 December 2009; Revised 12 May 2010; Accepted 2 June 2010

ABSTRACT: Floodplain deposition is an essential part of the Holocene sediment dynamics of many catchments and a thorough dating control of these floodplain deposits is therefore essential to understand the driving forces of these sediment dynamics. In this paper we date floodplain and colluvial deposition in the Belgian Dijle catchment using accelerator mass spectrometric radiocarbon and optical stimulated luminescence dating. Relative mass accumulation curves for the Holocene were constructed for three colluvial sites and 12 alluvial sites. A database was constructed of all available radiocarbon ages of the catchment and this database was analysed using relative sediment mass accumulation rates and cumulative probability functions of ages and site-specific sedimentation curves. Cumulative probability functions of ages were split into different depositional environments representing stable phases and phases of accelerated clastic deposition. The results indicate that there is an important variation between the different dated sites. After an initial stable early and middle Holocene phase with mainly peat growth in the floodplains, clastic sedimentation rates increased from 4000 BC on. This first phase was more pronounced and started somewhat earlier for colluvial deposits then for alluvial deposits. The main part of the Holocene deposits, both in colluvial and alluvial valleys, was deposited during the last 1 ka. The sedimentation pattern of the individual dated sites and the catchment-wide pattern indicate that land use changes are responsible for the main variations in the Holocene sediment dynamics of this catchment, while the field data do not provide indications for a climatological influence on the sediment dynamics. Copyright © 2011 John Wiley & Sons, Ltd.

KEYWORDS: dating; alluvium; colluvium; Holocene; land use change; climate change.

Introduction

Soil erosion, sediment transport, deposition and redistribution are important geomorphological processes during the Holocene in many temperate regions. A large number of studies have indicated the strong link between anthropogenic land use and soil erosion and colluvial deposition, while also climatic events may have a determining influence (e.g. review in Dotterweich, 2008). These driving forces can also have an important influence on sediment storage in floodplains (e.g. Trimble, 2009; Verstraeten *et al.*, 2009a), while river systems and floodplains may also buffer the influence of such catchment perturbations for the downstream parts of the catchment (e.g. Knox, 2006; Walling *et al.*, 2006). Over time spans of centuries to millennia, river systems are not only transporting sediment but also play an important role in the storage of sediments: floodplain sedimentation often makes up an important fraction of the total eroded sediment, and the combined amount of sediments stored as colluvium and in floodplains most often exceeds the amount of sediment exported from catchments of at least some square kilometres (e.g. Hoffmann *et al.*, 2007; Rommens *et al.*, 2006). In the perspective of the transition from nature-dominated to human-dominated environmental changes during the Holocene (e.g. Messerli *et al.*, 2000; Meybeck, 2003), the changing influence of anthropogenic land use and climatic variations on the sediment dynamics is of particular interest. Holocene climatic and land cover variations have caused large variations in sediment dynamics in many temperate regions, but the individual contribution of both factors to the variations in the sediment dynamics is often difficult to quantify.

Establishing links between forcing factors and sediment deposition relies on an accurate and detailed dating control of floodplain deposition. Dating of floodplain deposits is, however, often problematic, e.g. due to the unavailability of datable material or methodological problems with the used dating techniques (Verstraeten *et al.*, 2009b). Dating of floodplain sediments is often based on radiocarbon dating, although there are recent developments in the dating of sediment chronologies using optical dating and the application of terrestrial nuclides (e.g. Lang, 2008). One of the major problems with radiocarbon dating is the unavailability of datable material in many floodplain deposits, leading to low temporal resolutions. Several approaches have been applied to enhance the use of radiocarbon dating: statistical analysis of radiocarbon dates (e.g. Macklin and Lewin, 2003; Hoffmann *et al.*, 2008) and derivative parameters (e.g. Hoffmann *et al.*, 2009), and the use of replicate samples for accuracy testing and Bayesian modelling of resulting probability distributions (e.g. Chiverell *et al.*, 2009).

Verstraeten *et al.* (2009b) stress the importance of establishing precise chronologies and the construction of temporally differentiated sediment budgets in order to derive the relationships between environmental variability and sediment dynamics. Such budgets are the accounting of sources, sinks and pathways of sediment (Reid and Dunne, 2003; Slaymaker, 2003). According to Foulds and Macklin (2006), sediment budgeting is a necessary tool to understand the role of land use change on catchment stability, as it identifies reach-scale zones of sediment transfer and storage. Several studies have constructed catchment-wide sediment budgets for relative short periods ranging from days to a few decades (e.g. Beach, 1994; Page *et al.*, 1994; Fryirs and Brierley, 2001; Trimble, 1983, 1999; Walling and Quine, 1993; Walling *et al.*, 2002, 2006), while other studies have concentrated on long-term sediment budgets (e.g. spanning the entire Holocene). Only few studies have constructed a time-differentiated sediment budget for periods covering at least the period since the introduction of agriculture (e.g. de Moor and Verstraeten, 2008; Trimble, 2009; Verstraeten *et al.*, 2009a). Such time-

*Correspondence: Bastiaan Notebaert, Division of Geography, Department of Earth and Environmental Sciences, KU Leuven Celestijnenlaan 200E, 3001, Heverlee, Belgium.
E-mail: bastiaan.notebaert@ees.kuleuven.be

differentiated sediment budgets provide insight into the temporal and spatial variability in sediment fluxes, allowing more robust relationships between driving forces and the sediment dynamics.

The objective of this paper is to date sediment deposition in alluvial and colluvial environments in the medium-scaled Dijle catchment (758 km^2), located in the central Belgian Loess Belt. Radiocarbon dating and optically stimulated luminescence (OSL) dating are used and evaluated. Based on the available dates, a catchment-wide pattern of sedimentation is derived and this is being qualitatively linked to environmental changes as driving forces. Finally, the available dates are combined with an existing Holocene sediment budget (Notebaert *et al.*, 2009) in order to construct a time-differentiated sediment budget. This sediment budget can be used to establish quantitative relationships between the environmental changes and variations in sedimentation rates.

Study area

Within this study the Dijle catchment upstream of Leuven (758 km^2) is considered (Fig. 1). The catchment consists of a loess-covered undulating plateau ranging between 80 and 165 m above sea level (a.s.l.), in which river valleys have incised. There is a long history of land use, with first traces of agriculture from the Atlantic Period (ca. 5800–3000 BC), and intensive anthropogenic land use during the Roman Period and from the Middle Ages on. A more detailed description of the catchment can be found in Notebaert *et al.* (2009). The fluvial architecture of the Dijle catchment indicates that overbank deposition in floodplains is the most important Holocene process (Notebaert, 2009). Floodplain and backswamp sediments are loamy and silty, while point bar and river bed sediments are sandy. The sandy sediment which is related to the lateral migration of the riverbed is limited to parts of the floodplain, and the majority of the floodplain consists of a continuous aggradation profile.

Methods

Corings were located along cross-sections through the floodplain (Notebaert, 2009), and cross-sections and corings were selected for dating using several criteria: representativeness according to the local fluvial architecture, suitability to date floodplain aggradation and availability of datable material. Accelerator mass spectrometry (AMS) radiocarbon dating and OSL dating were combined and typically one coring per cross section was dated. Corings were selected based on their suitability to provide insight into net floodplain aggradation: they lack traces of erosional boundaries or river channel and point bar deposits, and thus represent continuous Holocene aggradation profiles. Based on the available OSL and radiocarbon ages, sedimentation curves are constructed for the individual dated sites. The available sedimentation rates were transformed into mass accumulation rates, giving the mass accumulation per floodplain or colluvial valley area, by applying a bulk density value and correcting for the presence of organic material (see below). Next, these mass accumulation curves where normalised by the total Holocene deposited mass at the study site in order to allow direct comparison between the different dated sites.

AMS radiocarbon dating

Samples for radiocarbon dating were taken using hand augering, percussion drilling and profile pits. In this study in total 12 sites were dated using radiocarbon and OSL dating, ranging from small colluvial valleys to the main alluvial plain. Colluvial deposits at two sites were dated in detail by Rommens *et al.* (2007) and Rommens (2006), yielding 12 dates. In this study detailed dating was performed at the Bilande site, with 18 radiocarbon dates. Dating of floodplain deposits is available from the Nethen catchment from Mullenders *et al.* (1966) and Rommens *et al.* (2006), with three and 10 radiocarbon dates respectively. De Smedt (1973) dated peat accumulation at one location in the main Dijle valley using five radiocarbon dates. Within this study, 44 samples were dated: one site (Korbeek-Dijle) was dated in detail, while for 10 other sites at least two samples were dated. In total 29 radiocarbon dates from colluvial deposits and 62 from alluvial deposits are available (see Fig. 1 for sampling locations). Except for the bulk samples, each sample was sieved and datable material was handpicked from the fraction larger than 125 μm. Terrestrial plant remains and wood were selected for dating, in order to avoid hard-water effects (e.g. Moor *et al.*, 1998) and reservoir effects (e.g. Törnqvist *et al.*, 1992). Resulting conventional radiocarbon

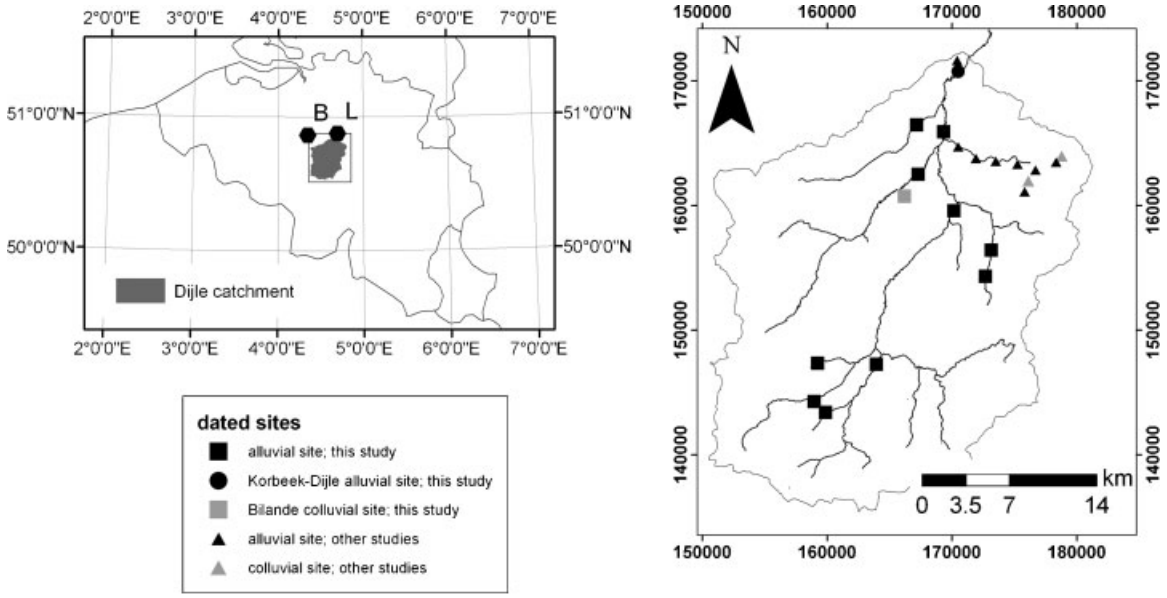

Figure 1. Location of the Dijle catchment within Belgium and sampling sites for radiocarbon and OSL dating in the Dijle catchment. B, Brussels; L, Leuven.

ages (BP) were calibrated using Oxcal 4.1 (Bronk Ramsey, 2001, 2009) and the Intcal 04 calibration curve (Reimer *et al.*, 2004). Calibrated ages are here referred to as 'cal a BP' (calibrated years before 1950) or as 'cal a' BC/AD or BC/AD, and uncalibrated ages as '^{14}C a BP'.

OSL dating

OSL dating was used for the floodplain of the Dijle River near Korbeek-Dijle. Sampling of OSL datable material was carried out with percussion drilling equipment, using PVC tubes of length 1 m and an inner diameter of 5 cm. The PVC tubes were opened in the laboratory under subdued orange light. Samples for luminescence analysis were taken about every 13 cm, with each collected sample representing a vertical interval of ~5–8 cm. In this manner, 32 samples were collected, of which 15 were selected for dating in the frame of this work. The samples were relatively fine grained, with grains in the range of 63–90 μm generally representing the coarsest fraction that was still practicable for luminescence analysis. Luminescence analysis was performed at Ghent University. Quartz grains from this fraction were extracted using conventional sample preparation techniques (HCl, H_2O_2, sieving, heavy liquids, HF). A sufficient amount of quartz grains could be extracted from 11 of the 15 samples. The purity of the quartz extracts was confirmed by the absence of a significant infrared stimulated luminescence (IRSL) response at 60°C to a large regenerative beta dose. The sensitivity to infrared stimulation was defined as significant if the resulting signal amounted to more than 10% of the corresponding blue light stimulated luminescence (BLSL) signal (Vandenberghe, 2004) or if the IR depletion ratio was not within 10% of unity (Duller, 2003).

For measurement, quartz grains were spread out on the inner 7 mm of 9.7 mm diameter stainless steel discs. The luminescence measurements were performed using an automated Risø-TL/OSL-Da-15 reader, equipped with blue (470 ± 30 nm) LEDs and IR (875 nm) diodes; all luminescence emissions were detected through a 7.5 mm thick Hoya U-340 UV filter. Details on the measurement apparatus can be found in Bøtter-Jensen *et al.* (2003).

The equivalent dose (D_e) was determined using the single-aliquot regenerative-dose (SAR) protocol (Murray and Wintle, 2000). Optical stimulation with the blue diodes was for 38 s at 125°C; the initial 0.3 s of stimulation was used in the calculations, minus a background evaluated from the following 0.5 s of stimulation. A preheat of 10 s at 180°C and a test-dose cut heat to 160°C were adopted; the preheat at 180°C was chosen to minimise thermal transfer (i.e. transfer of charge by heating from light-insensitive but thermally stable traps, into light-sensitive traps). After the measurement of each test dose signal, a high-temperature bleach was performed by stimulating with the blue diodes for 40 s at 280°C (Murray and Wintle, 2003). Measured aliquots were accepted if the recuperation and IRSL/OSL ratio did not exceed a threshold set at 10%, and if both the recycling ratio and the IR depletion ratio were within 10% of unity. The suitability of the experimental procedure was confirmed through a dose recovery test as outlined by Murray and Wintle (2003; see also Table 1). The overall ($n = 11$) average recovered to given dose ratio (± 1 standard error, σ) is 1.00 ± 0.01, which gives confidence in the reliability of the laboratory measurement procedure. For each sample, at least 15 replicate measurements of D_e were made.

The dosimetry (i.e. beta and gamma dose rates) is based on low-level gamma ray spectrometric analysis of sediment collected above and below each OSL sample, and used dose rate conversion factors derived from the nuclear energy releases tabulated by Adamiec and Aitken (1998). Water contents were

Table 1. Summary of radionuclide activity concentrations, estimates of the time-average water content (w.c.), calculated dose rates, D_e values, optical ages and dose recovery data for the OSL samples of the Korbeek-Dijle site in the Dijle catchment. The uncertainties mentioned with the dosimetry, D_e and dose recovery data are random; the uncertainties on the optical ages represent the total uncertainty, which includes the contribution from systematic sources of error (Aitken, 1985). All uncertainties are 1σ. The dose rate includes the contribution from cosmic rays and internal radioactivity. The number of aliquots used in luminescence analyses (D_e determination and dose recovery) is given in parentheses. Columns headed 'All aliquots' refer to values obtained by averaging the D_e over all aliquots; columns headed 'Aliquots rejected' refer to values obtained by calculating D_e following the procedure based on Fuchs and Lang (2001; see text for details). The dose recovery test consisted of bleaching fresh aliquots using blue diodes (2 × 250 s with a 10 ks pause in between), giving them a dose close to the expected natural dose, and measuring them using the SAR protocol.

									All aliquots		'Aliquots rejected'		
GLL code	Depth (cm)	^{238}U (Bq kg^{-1})	^{226}Ra (Bq kg^{-1})	^{210}Pb (Bq kg^{-1})	^{232}Th (Bq kg^{-1})	^{40}K (Bq kg^{-1})	w.c. (%)	Dose rate (Gy ka^{-1})	D_e (Gy)	Age (ka)	De (Gy)	Age (ka)	Dose recovery
081504	~30	36 ± 2	39 ± 2	32 ± 1	36.6 ± 0.4	458 ± 11	21 ± 5	2.44 ± 0.03	0.78 ± 0.07 (15)	0.32 ± 0.05	0.55 ± 0.03 (7)	0.23 ± 0.03	0.99 ± 0.05 (6)
081508	56	31 ± 2	40 ± 2	31 ± 3	40 ± 1	518 ± 5	38 ± 4	2.25 ± 0.04	1.5 ± 0.1 (17)	0.65 ± 0.07	1.17 ± 0.04 (11)	0.52 ± 0.04	0.95 ± 0.04 (6)
081512	80	31 ± 2	42 ± 2	35 ± 2	41 ± 1	534 ± 25	38 ± 4	2.32 ± 0.06	4.0 ± 0.5 (18)	1.7 ± 0.2	1.9 ± 0.2 (3)	0.8 ± 0.1	0.97 ± 0.02 (5)
081517	109	32 ± 2	38 ± 3	34 ± 1	36.9 ± 0.5	509 ± 8	38 ± 4	2.20 ± 0.02	4.2 ± 0.3 (17)	1.9 ± 0.2	2.7 ± 0.2 (4)	1.2 ± 0.1	1.01 ± 0.04 (6)
081521	144	32 ± 2	44 ± 9	36 ± 5	42 ± 9	603 ± 70	38 ± 4	2.48 ± 0.19	2.2 ± 0.2 (16)	0.9 ± 0.1	1.73 ± 0.04 (8)	0.70 ± 0.08	1.04 ± 0.02 (6)
081525	159	33 ± 4	34 ± 2	34 ± 2	36.8 ± 0.5	561 ± 13	38 ± 4	2.30 ± 0.03	2.1 ± 0.1 (17)	0.89 ± 0.08	1.75 ± 0.05 (9)	0.76 ± 0.06	1.04 ± 0.04 (4)
081532	220	38 ± 2	37 ± 2	34 ± 2	36 ± 1	493 ± 5	38 ± 4	2.15 ± 0.03	1.67 ± 0.07 (16)	0.78 ± 0.07	1.53 ± 0.04 (11)	0.71 ± 0.06	0.97 ± 0.03 (5)
081536	245	31 ± 3	39 ± 6	37 ± 8	40 ± 9	565 ± 75	38 ± 4	2.36 ± 0.21	2.6 ± 0.2 (17)	1.1 ± 0.2	1.88 ± 0.06 (6)	0.8 ± 0.1	0.96 ± 0.03 (6)
081542	282	37 ± 3	47 ± 5	42 ± 2	39 ± 1	458 ± 31	38 ± 4	2.19 ± 0.07	2.56 ± 0.06 (19)	1.2 ± 0.1	2.12 ± 0.08 (3)	0.97 ± 0.09	1.00 ± 0.02 (6)
081549	378	38 ± 2	49 ± 2	41 ± 1	44 ± 1	548 ± 73	38 ± 4	2.42 ± 0.16	4.9 ± 0.1 (18)	2.0 ± 0.2	4.8 ± 0.1 (16)	2.0 ± 0.2	1.02 ± 0.03 (6)
081567	579	12 ± 2	14 ± 3	13 ± 1	10.9 ± 0.4	181 ± 4	24 ± 3	0.90 ± 0.02	24.7 ± 0.7 (19)	27 ± 2	23.7 ± 0.5 (16)	26 ± 2	1.00 ± 0.03 (6)

derived from laboratory measurements of saturated samples. The uppermost sample, taken at 0.3 m depth (GLL-081504, see Table 1), was assumed to have been saturated with water for 50% of its burial period; for the remainder of the samples, the time-averaged moisture content was estimated to be equal to 90% of the saturation content. The contribution from cosmic rays was calculated following Prescott and Hutton (1994), and an internal dose rate of 0.010 ± 0.002 Gy ka^{-1} was adopted (Vandenberghe *et al.*, 2008).

Sediment mass accumulation rates

Sedimentation rates ($SR_{i,obs}$) are normally calculated for each sample of the radiocarbon database using the following equation:

$$SR_{i,obs} = (D_i - D_{i\text{-}1})/(T_i - T_{i\text{-}1}) \quad (1)$$

with D_i and T_i the depth and age of the sample and D_{i-1} and T_{i-1} the age and depth of the stratigraphic following (younger) sample. However, this approach has some drawbacks. Firstly, the above calculated sedimentation rates represent total floodplain accumulation rates, including both clastic sedimentation as well as organic sedimentation (peat growth and organic-rich sediments). Especially for the Dijle floodplain, where large variations occur in the organic matter concentrations within and between corings, a correction needs to be made in order to obtain clastic sediment mass accumulation rates. Secondly, at some floodplain locations more sediment has been deposited during the entire Holocene than at other locations, thus resulting in higher sedimentation rates. This site dependence on sedimentation rates makes it troublesome to identify periods with higher or lower sedimentation rates, especially when available sediment datings are retrieved from a variety of locations. Therefore relative Holocene floodplain mass accumulation rates were calculated. These are defined as the fraction of sediment mass per unit floodplain area deposited after the moment of sample deposition compared to the total Holocene sediment accumulation for the considered coring. The use of relative amounts allows a more straightforward comparison of corings with different total Holocene sediment accumulation. The resulting relative sedimentation rates were plotted vs. age for the different dated corings, giving a first insight into the sedimentation history of the catchments. Separate relationships were constructed for colluvial and alluvial ages, the last group containing both dates from floodplain fines and peat and organic rich layers but excluding the river channel and point bar deposits.

In order to calculate these relative sediment mass accumulation rates, floodplain sediments were first divided into three units. Comparable to Rommens *et al.* (2006), soil units were in-field classified into three OM classes: clastic deposits, organic deposits and peat layers. The thickness of these units was converted into mass of sediment using (Verstraeten and Poesen, 2001)

$$M_{layer,i} = d_{layer,i} \frac{1}{\frac{1}{DBD_{MS}} + \frac{OM}{(1-OM)DBD_{OM}}} \quad (2)$$

with $M_{layer,i}$ the sediment mass (mg) per m^2 floodplain area of layer i, $d_{layer,i}$ the thickness of layer i (m), OM the percentage organic matter of the unit to which the layer belongs, DBD_{OM} the dry bulk density of the organic matter (mg m^{-3}) and DBD_{MS} the dry bulk density of the clastic component (mg m^{-3}). Values for OM were determined for 14 samples by using the combustion method (e.g. Bisutti *et al.*, 2004) combined with data from Rommens *et al.* (2006), whereas the values for DBD were taken from Rommens *et al.* (2006) ($DBD_{OM} = 0.35$ mg m^{-3}; $DBD_{MS} = 1.42$ mg m^{-3}). Based on the laboratory results, average OM% values of 4%, 8% and 70% were defined for clastic deposits, organic deposits and peat layers. Although we recognise that the use of such averaged values introduces an additional error, we believe that these corrections are necessary to come to realistic accumulation rates.

Additionally, the total mass per unit floodplain area of sediment that was deposited after the deposition of the dated material (M_{sample}, mg m^{-2} floodplain area) was calculated for each sample using

$$M_{sample} = \sum_{i=1}^{n} M_{layer,i} \quad (3)$$

with n the number of alluvial sedimentary layers situated above sample s, and deposited since deposition of the sample up to the present, and $M_{layer\ i}$ the mass of layer i (mg m^{-2} floodplain area) calculated using equation (2). The entire mass per unit floodplain area (M_{coring} in mg m^{-2} floodplain area) can also be calculated for each coring. The relative mass ($M_{relative}$, %) of sediment accumulation after the deposition of the sample up to the present can be compared to the mass of the total Holocene sediment accumulation using

$$M_{relative} = M_{sample}/M_{coring} \quad (4)$$

The relative mass accumulation rate (MR, % a^{-1}) for sample i can then be calculated using

$$MR_i = (M_{relative,i} - M_{relative,i\text{-}1})/(T_i - T_{i\text{-}1}) \quad (5)$$

with T_i the time since deposition, and index $i-1$ corresponding to the stratigraphic younger sample deposited above this deposit. In order to compare samples from different corings with different sampling and dating densities, the relative mass accumulation and sedimentation rate are calculated compared to the present, thus setting $T_{i-1} = 0$, from which follows $M_{relative,i-1} = 0$ and $D_{i-1} = 0$.

Hoffmann *et al.* (2009) calculated sedimentation rates and applied models to evaluate these sedimentation rates. Therefore we also compared our MR curves with modelled values, using five scenarios. Based on the analysis results, each scenario starts with an MR of 0.001% a^{-1} at 10 000 BC, followed by a linear increase of the MR from a given date to the present. The linear increase is fitted in such a way that the total accumulated relative mass accumulation ($M_{relative,total}$) equals 100%:

$$M_{relative,total} = \sum_{i=-12000}^{0} MR_i = 100\% \quad (6)$$

with i the considered age with an interval of 1 AD. As a result, the maximal MR_i will depend upon the onset of the increase in sedimentation. Scenarios were simulated with a linear increased MR starting at 2000 BC, 1000 BC, 1 AD, 500 AD and 1000 AD. The scenarios were evaluated using the Nash and Sutcliffe model efficiency (ME) statistic (Nash and Sutcliffe, 1970). The applied scenarios all yield an identical total mass accumulation (100%), while the early Holocene mass accumulation is also constant (0.001% a^{-1}), which means that the magnitude of the accumulation for the most recent periods will depend on the length of the period with increased sedimentation. This is in contrast to the scenarios calculated by Hoffmann *et al.* (2009) which use a constant sedimentation rate of 0.03 cm a^{-1} for the early and mid Holocene period, followed by a linear increase to 0.4 cm a^{-1}, with a start of this increase at 1000 BC, 500 AD or 1800 AD. Depending on the moment of the start of the linear increase, the total sedimentation (mm) will vary, with a larger total sedimentation when the increase starts earlier. Our method avoids the differences in total sediment accumulation between the different models.

Cumulative probability distributions

Recently, several studies use cumulative probability distributions (CPDs) of radiocarbon ages obtained from alluvial and/or colluvial deposits for the analysis and comparison of Holocene fluvial dynamics within Europe. Techniques were compiled and applied on data from Great Britain (e.g. Macklin and Lewin, 2003; Lewin *et al.*, 2005) and later applied in Poland (Starkel *et al.*, 2006), Spain (Thorndycraft and Benito, 2006a,b), Germany (Hoffmann *et al.*, 2008) and in the Rhine catchment (Hoffmann *et al.*, 2009). A comparison is also made between datasets obtained from Great Britain, Poland and Spain (Macklin *et al.*, 2006). For the analysis of German datasets (Hoffmann *et al.*, 2008) several methodological improvements were introduced. The radiocarbon ages used are grouped in a different way: where Lewin *et al.* (2005) focus mainly on changes in fluvial style or sedimentation rates, Hoffmann *et al.* (2008) calculate frequency distributions of ages which are yielded from deposits corresponding to active sedimentation phases. Hoffmann *et al.* (2008) argue that this results in a better proxy of the response to external impacts. The frequency distributions of German dates were also normalised, which limits the effects of the calibration curve, different preservation potentials and sampling bias. Recently Macklin *et al.* (2010) further improved the analysis of the frequency distributions of radiocarbon ages from the UK.

In this study a database of radiocarbon ages from the Dijle catchment was compiled, holding all available radiocarbon dates from colluvial and alluvial deposits, based on this study and previous studies (Mullenders *et al.*, 1966; De Smedt, 1973; Rommens, 2006; Rommens *et al.*, 2006). Radiocarbon ages which are considered problematic in the original publication are not included in the database. The ages of this database were grouped and for the different groups cumulative probability distributions (CPDs) were constructed by the addition of the probability functions of the individual calibrated radiocarbon ages. A distinction was made between different sedimentary facies (e.g. Hoffmann *et al.*, 2008): colluvial deposits, floodplain fines (overbank deposits), river channel and point bar deposits, and peat and organic-rich layers. Samples from channel and point bar deposits are not included in this analysis due to the low number of dated samples (Table 2). These facies types were then again grouped in terms of their fluvial activity (Table 3; based on Hoffmann *et al.*, 2008): the first two are considered to represent phases of active colluvial or alluvial sediment deposition; the last one is considered to represent phases of relative stability in the clastic floodplain accumulation phases. Most sampling of peat and organic-rich layers occurred at the bottom or the top of these layers, in order to date the transition between clastic and organic floodplain accumulation, which can bias the distributions of peat ages.

The shape of the calibration curve used also has an influence on the resulting CPDs. This effect is illustrated by the CPD of 100 equally spaced ages with an (uncalibrated) standard deviation of 45 a. The used standard deviation of 45 a equals the average standard deviation of the radiocarbon ages in the database. Each of the calculated CPDs can be divided by the CPD of equally spaced ages in order to correct for the effects of calibration curve (Hoffmann *et al.*, 2008). Alternatively, a correction can be made by dividing a CPD by the CPD of all available ages (Hoffmann *et al.*, 2008). As preservation potential does not present a problem for the samples of the Dijle catchment due to the sampling techniques, where only samples were taken from corings with a continuous aggradation profile during the Holocene, this method was not applied here. Only for colluvial depots might the preservation potential play a role, as sedimentary evidence for intact aggradational colluvial archives is not available. Apart from the problems with the calibration curve and the preservation potential, other limitations may arise with the methodology used (Hoffmann *et al.*, 2008), related to the variable precision of radiocarbon ages and the possible time difference between the age of deposition and the age of the dated material.

Table 2. Groups of sedimentary facies, available number of radiocarbon ages and number of radiocarbon ages used for the analysis of radiocarbon ages in the Dijle catchment.

Sedimentary facies	Number of ^{14}C ages	Number of ages used
Colluvial deposits	29	21
Floodplain fines (overbank deposits)	10	10
River channel and point bar deposits	1	1
Peat and organic rich layers	51	49
Top of peat layer	19	19
Bottom of peat layer	13	12
Total	91	81

Table 3. Different activity groups, available number of radiocarbon ages and number of radiocarbon ages used for the analysis of radiocarbon ages in the Dijle catchment.

Activity group	Number of ^{14}C ages	Number of used ages
Aggradation	39	31
Stability	51	49

Time-differentiated sediment budget

A Holocene sediment budget was previously constructed for the Dijle catchment (Notebaert *et al.*, 2009). A detailed description of the methodology can be found in Notebaert *et al.* (2009). The calculations were adapted in this study to the more accurate measurements of organic matter content of the peat layers which are mentioned above. In order to get a deeper insight into the sediment dynamics of a catchment, it is important to incorporate also the temporal dynamics of the system. Based on the available ages, and comparable with other studies (e.g. Trimble, 1999, 2009; de Moor and Verstraeten, 2008; Verstraeten *et al.*, 2009a), the sediment budget was differentiated in three time periods: early Holocene to 2000 BC, 2000 BC to 1000 AD and 1000 AD to present. These periods were selected based on the sedimentation history of the catchment. A more detailed time differentiation of the sediment budget would require a more detailed dating of the alluvial and colluvial deposits.

The time differentiation of sediment deposition is based on the relative mass accumulation rate (MR, equation (5)) for the dated sites. Based on the site-specific values, a weighted average mass accumulation for each period was calculated for the trunk valley, tributary valleys and the colluvial valleys. Only (dated) sites were used where a date was available within a time frame of ca. 1000 a (for 2000 BC) or ca. 500 a (for 1000 AD) from the starting date of the considered time periods. Sites where no dates for these start points are available but where the uncertainty on the relative accumulated mass for these points is smaller than 10%, e.g. due to a small relative mass accumulation increase between two available dates, are also used. In this way the averaging effects between the dated points are minimised. Weighting was based on the floodplain width and Holocene sediment thickness. The selecting of sites and weighting result in a difference in the catchment averaged sedimentation curve compared to a pure mathematical curve.

Dating information is only available for deposition environments, while temporal information on the sediment sources (erosion rates) and catchment export is absent. In order to come to a catchment-wide budget incorporating these sources and sinks, some assumptions are required:

1. Verstraeten *et al.* (2009a) assume that catchment export follows the same trends as floodplain storage. They state that sediment deposition is controlled by inundation frequency and sediment concentration – factors which also control sediment yield. As a result, periods with higher floodplain storage will also be periods with higher export from the catchment. For the Dijle catchment it is demonstrated that floodplain storage was very low during the early and mid Holocene, while during this same period a fixed river channel is absent and water is transported in a diffuse way over a broad floodplain, without forming typical river bed deposits (De Smedt, 1973). Such a diffuse water transport is most probably accompanied by very low sediment export rates.
2. For each period mass is preserved. As a result the sediment production equals the sum of the export and the colluvial and alluvial storage.
3. As no dates are available for sediment deposition on the hillslopes (excluding colluvial valley deposition), the temporal framework for this sink should be based on some assumptions. This hillslope sediment deposition can be assumed to follow an equal trend as sediment deposition in the colluvial valleys. This is the first scenario ('scenario 1') that is calculated. For the Nethen catchment, however, Verstraeten *et al.* (2009a) argue that this would result in an unrealistic sediment delivery ratio of nearly 100% for the period before colluvial deposition starts (early Holocene). Modelling results in the Geul catchment (de Moor and Verstraeten, 2008) show indeed a high sediment delivery ratio for the early and mid Holocene, but still much lower than 100%. Therefore, scenario 2 was developed by assuming that sediment deposition on the slopes is assumed to follow the same trend as the combined storage in colluvial and alluvial deposits, an approach which yielded more realistic values in the Nethen catchment according to Verstraeten *et al.* (2009a).

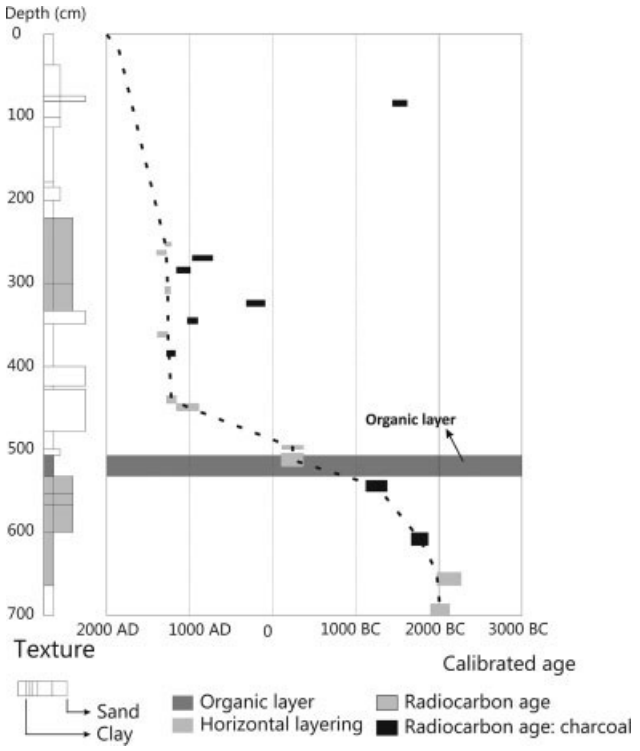

Figure 2. Overview of the coring data at Bilande (Dijle catchment) with radiocarbon dates. Sampling depths and calibrated radiocarbon ages are plotted on the right. Boxes indicate the calibrated radiocarbon ages with a 2σ error: black boxes are ages based on charcoals; grey boxes are ages based on terrestrial plant remains and wood. The dashed line indicates the suggested sedimentation history. The width of the boxes in the left column varies with the texture. The presence of two boxes indicates an alternation of fine layers with different texture. Layering is indicated by a light-grey filling; organic deposits are indicated by dark-grey filling.

Results

Dating floodplain and colluvial accumulation

In this study the colluvial valley at Bilande (for location see Fig. 1) was dated in detail. In total 16 samples were dated using radiocarbon dating and sample depth is plotted against calibrated age in Fig. 2. Radiocarbon dating performed on charcoal samples or samples containing both charcoal and terrestrial plant remains or wood is problematic: six out of eight samples show an age–depth inversion. Possibly the two lower charcoal-based dates suffer also an age–depth inversion, but sampling and dating resolution is insufficient for conclusions. The overestimation of age for those charcoal dates can easily be explained by the cascade model of colluvial formation (Lang and Hönscheidt, 1999). This implies that older colluvial deposits have been eroded, and material from these older colluvial deposits is thus reworked and again deposited at their current location.

The dating from the Bilande site shows two important sedimentation phases and one stability phase: a first sedimentation phase starts around 2000 cal a BC and is followed by the formation of an organic layer of which the top is dated around 1 AD. Parts of this first depositional phase show layers, indicating that it does not originate from a single event. After the formation of the organic layer again clastic sediment was deposited. Between 1 AD and about 1000 AD, sedimentation rate appears to be low, although this can be caused by the limited dating resolution, which causes an averaging effect. A major sedimentation phase occurred between 1230 AD and 1295 cal a AD (1σ calibrated interval, 1150–1450 cal a AD on a 2σ interval), with the deposition of at least 1.87 m sediment. Some parts of these deposits show layering, including small (1–3 mm) layers containing plant remains and traces of *in situ* growing plants, indicating that this depositional phase is not caused by a single event. Due to the absence of dates in the upper part of the coring, the extent of this major deposition phase and the subsequent deposition rates cannot be derived. Drainage tubes from ca. 1846 AD are located at a depth of 0.4–0.6 m, indicating that deposition in the last 150 a was less than 0.2 m.

Dating results of the floodplain of the Dijle near Korbeek-Dijle (for location see Fig. 1) are represented in Fig. 3. Table 1 summarises the results from D_e and dose rate determination of the OSL dating, and shows the calculated optical ages (see also Fig. 4, squares). It can be seen that not all age results are consistent with the stratigraphic position of the samples. We interpret this inconsistency as indicative for incomplete resetting of the OSL clock in the quartz grains. A large spread in D_e values was observed for the majority of the samples, with relative standard deviations ranging from ~20% (sample GLL-081532) to 50% (sample GLL-081512). This also indicates that the aliquots consist of a mixture of grains which have been reset to various degrees. Interestingly, the variability is already

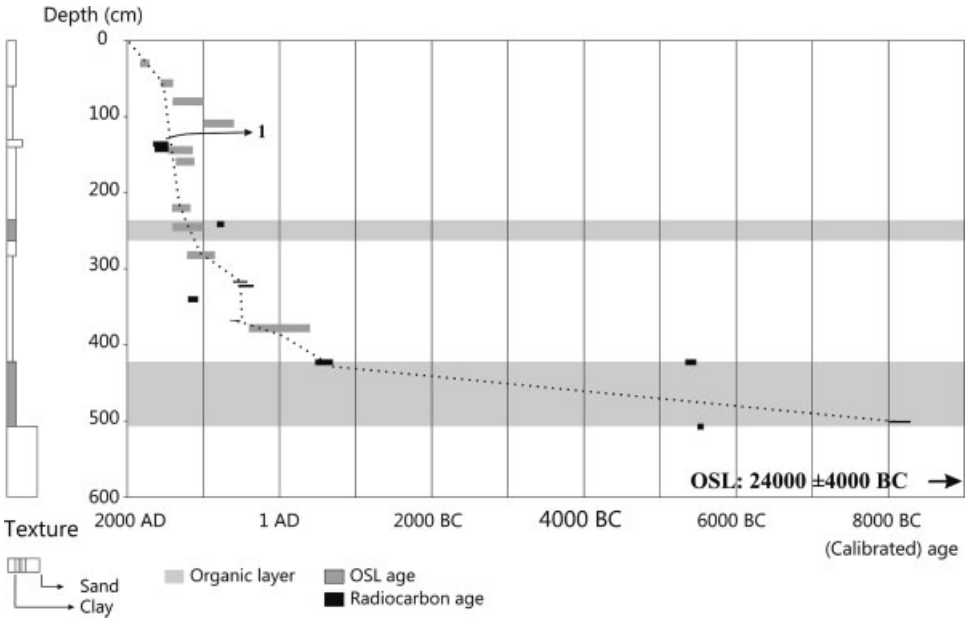

Figure 3. Overview of the coring data at Korbeek-Dijle (Dijle catchment) with radiocarbon and OSL dates. Peat layers are indicated by grey shading. Boxes indicate ages with a 2σ error: black boxes indicate radiocarbon ages; light-grey boxes indicate corrected OSL ages. A radiocarbon date obtained from charcoal is indicated by '1'. The dashed line represents the proposed sedimentation history.

observed for large (i.e. 7 mm diameter) aliquots, which may imply that only a small fraction of the grains contributes to the measured luminescence. The D_e values for the three lowermost samples (samples GLL-081542, -49 and -67) have a higher accuracy, with values of the relative standard deviation in the range of 9–13%. For sample GLL-081532, the relative standard deviation of the D_e data is 16%. As all samples exhibit a similar overall luminescence sensitivity, this variability in precision indicates that resetting in the lowermost samples was more homogeneous (and possible more complete), and/or that they contain more grains that contribute to the measured signal, with each grain emitting less intense luminescence (so that grain-to-grain variations are averaged out to a greater extent). As the uppermost 4–5 m of sediment is probably derived from the same source, samples GLL-081504 to -49 are expected to exhibit the same material characteristics. Therefore, the value of the relative standard deviation is taken as a measure for the degree of resetting.

Fuchs and Lang (2001) suggested a procedure to improve D_e determination in incompletely reset samples using a limited amount of replicate measurements. This procedure consists of arranging the D_e values in ascending order, and calculating a running mean (starting with the two lowermost D_e values) until

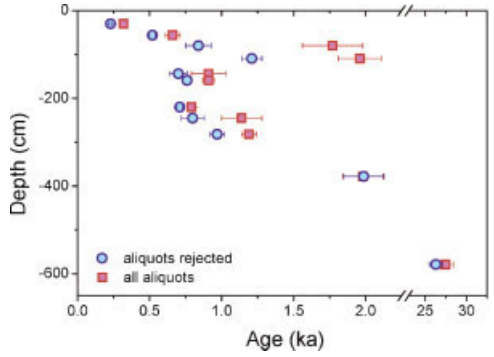

Figure 4. Plot of age vs. depth for the OSL ages at Korbeek-Dijle (see also Fig. 3). The error bars represent the overall random uncertainty (1σ) only. As such, the figure allows evaluation of the internal consistency of the optical ages. The squares refer to ages based on the mean D_e over all measured aliquots; the circles refer to the ages obtained after rejecting D_e values following a procedure similar to the one proposed by Fuchs and Lang (2001; see text for details). This figure is available in colour online at wileyonlinelibrary.com.

the relative standard deviation exceeds the value of what is defined as the precision of the method. We applied this procedure to our dataset, with the precision of the measurement method being defined as that observed in the dose recovery tests. The resulting ages are shown in Fig. 4 (circles; see Table 1 for the analytical data). It can be seen that the OSL ages are now stratigraphically more consistent, with the dataset containing only one clear outlier (sample GLL-081517).

Concerning the D_e selection procedure outlined above, it should be pointed out that (i) it may yield ages that still overestimate the true burial age (as they are derived from OSL signals originating with more than one grain), (ii) it assumes that the precision obtained in measurements of artificially bleached and irradiated aliquots accurately represents the precision that would be observed for well-bleached natural samples, and (iii) it assumes that also a very limited number of replicate measurements yields a reliable estimate for the burial dose. These considerations should be taken into account when interpreting the age results and limit the conclusions that can be drawn.

The ages obtained for the three lowermost samples (GLL-081542 and -49 situated in overbank or backswamp silts and GLL-081567 situated in the braided river sandy deposits) are based on the most reproducible measurements of the D_e. The date of 23.7 ± 0.5 ka for sample GLL-081567 confirms the presumed Late Pleistocene age of the sandy braided river deposits below the peat layer. The set of OSL ages for the overlying unit suggests that it was deposited in at least two distinct phases. A first phase comprises the sediments at a depth of ~4 m to ~3 m, which were deposited between 2.0 ± 0.2 ka (sample GLL-081549) and before ~1 ka ago (sample GLL-081542). A second phase is characterised by a significantly higher sedimentation rate, as the uppermost 3 m of sediment must have been deposited in less than 1 ka.

We hypothesise that more heterogeneous resetting of the luminescence signal in the uppermost samples gives an indication for a high sedimentation speed. A high sedimentation speed lowers the probability for all grains to have their luminescence signal reset at the moment of deposition.

The depositional and sedimentary history of the Korbeek-Dijle site shows formation of a basal peat layer between ~8000 BC and ~500 BC. It is unclear whether a second date of the top of the peat layer giving ~5000 BC is correct, as this date is obtained from a bulk sample and reworking of peat cannot be

excluded. A subsequent sedimentation phase ends around 1100 AD, with a major sedimentation period around 500 AD. Of the three samples yielding ages of ~500 AD, the deepest one is yielding the oldest uncalibrated age, but they are overlapping on a 2σ calibrated interval. The top of a second peat layer is dated by radiocarbon dating around 900 AD and by OSL dating around 1200 AD. The OSL age is considered to be more accurate: the radiocarbon date is obtained from a bulk sample, with possibly age overestimation due to reservoir effects and radiocarbon dates not obtained from bulk samples of comparable peat layers at other locations yield ages between 1000 and 1400 AD. The main sedimentation phase at Korbeek-Dijle is situated after the formation of this peat layer. This phase suffers from a low dating resolution. However, we discussed that the heterogeneity of the luminescence signal resetting gives an indication for high sedimentation rates. Additionally, when assuming that the error on the luminescence ages with rejected aliquots gives a good indication of the real age, it can be argued that sedimentation is concentrated around 0.6–0.8 ka ago, with the deposition of 1.6–1.8 m sediments. This implies that during the last 500 a only about 0.6 m of sediment is deposited.

Catchment-wide pattern of floodplain and colluvial deposition

Figure 5 plots the age and relative accumulated mass per unit depositional area for the colluvial sites, whereas Fig. 6 provides this information for alluvial sites. Based on Fig. 6 the average accumulated sediment mass for the tributaries and main trunk floodplain was calculated (Fig. 7). The calculated rates are not corrected for the dating resolution of the different sites and are therefore influenced by averaging effects.

Data for the colluvial sites show the start of deposition between ~4160 BC and ~600 BC, while the main accumulation of sediment mass occurred for all sites in the last 3 ka (Fig. 5). During the last ca. 1 ka between 60% and 30% of the sediment mass accumulation took place. As for most alluvial sites only two or three dates are available, these curves suffer largely from an averaging effect and interpretation should consider this averaging. Within the alluvial graphs (Fig. 6) one major outlier is apparent: at the site Bonlez U almost all sedimentation took place before ca. 1400 BC. After the early and mid Holocene aggradation phase the river incised the floodplain to a depth of ~6 m (Notebaert, 2009). The only dating control on this incision phase is the age of the top of the floodplain (ca. 1400 BC). This site has an important influence

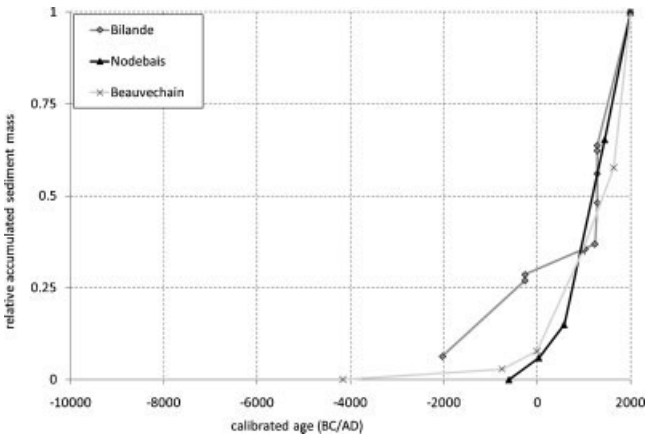

Figure 5. Age and relative accumulated sediment mass for the different dated corings in colluvial deposits in the Dijle catchment. Data for the Nodebais are reported by Rommens *et al.* (2006) and data for the Beauvechain site by Rommens (2006).

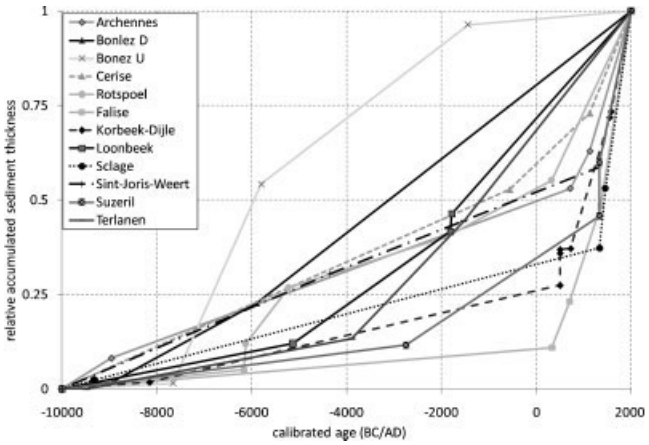

Figure 6. Age and relative accumulated sediment mass for the different dated corings in alluvial deposits in the Dijle catchment. Data for Rotspoel are obtained from De Smedt (1973). A value of 70% is used for the percentage of organic matter in the peat layers.

on the average values calculated for the tributary floodplains (Fig. 7). For sites where the first Holocene floodplain accumulation is dated, this phase is situated between 10 000 and 8000 BC. Mass accumulation before 500 BC is rather limited for most sites, although there is a wide scatter. Most sites show a first increase in sediment accumulation between 4000 BC and 500 BC, with again a high scatter. A second increase in sediment accumulation is observed for most sites around 1000 AD.

Due to the averaging effect and the rather low resolution of the dates, it is not possible to identify short-term variations in sediment accumulation, and thus it is not clear how long the sedimentation phases lasted, or what the intensity of the phases was. The possibility of intermediate periods with less accumulation cannot be excluded. The presence in most cross-sections of a peat layer within the upper clastic layer (e.g. Korbeek-Dijle site, see above) suggests a stable phase. Ages for this peat layer range between 700 and 1400 AD.

The average relative sediment mass accumulation (Fig. 7) provides an overview of the catchment-wide sedimentation patterns. These averages are, however, still largely influenced by single dated cross-sections, as indicated by the influence of the Bonlez U cross-section. These averaged values indicate that

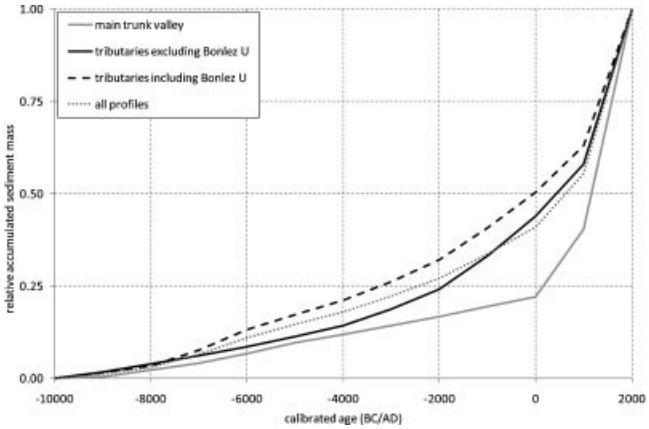

Figure 7. Age and average relative accumulated sediment mass for the different dated corings in alluvial deposits in the Dijle catchment. Average values are calculated for the main trunk valley, tributaries, tributaries excluding the dates from the Bonlez U cross-section and for all cross-sections. A value of 70% is used for the percentage of organic matter in the peat layers.

deposition in the trunk valley floodplain is mainly concentrated in the last 1–2 ka. Deposition in the tributary floodplains increased earlier than in the trunk valley floodplain, with an important increase starting around 2000 BC. This pattern is, however, influenced by averaging effects caused by the dating resolution. To make a correct interpretation of the sedimentation history for the trunk valley floodplains, for each time frame only sites should be included with a sufficient temporal dating resolution for the considered period.

Analysis of sedimentation rates

The plots of sedimentation rates (SR) and the relative mass accumulation rates (MR) (Fig. 8) show rather constant SR and MR values before 4000 BC, slightly increasing values between 4000 BC and 1000 BC, and then more increasing values after 1000 BC, while also the scatter increases. Model efficiency values for several sedimentation rate scenarios were compared with these plots (Table 4). For the fluvial ages ME was also calculated excluding the dates of Bonlez U (Table 4; see above). ME is highest for the model with increased colluvial sedimentation starting at 1000 BC and alluvial sedimentation at 1 AD. However, from the pattern of floodplain and colluvial deposition it is clear that such scenarios are an oversimplification of the real sedimentation history as these do not incorporate several phases of increased or decreased sedimentation. Nevertheless, the models give an indication of a time lag between the start of increased sedimentation in colluvial and alluvial deposits.

An increase in sedimentation rate with a decreasing measuring period is reported for many sedimentary deposits, and this phenomenon has been linked to a time dependency in sediment accumulation rates (e.g. Sadler, 1981; Schumer and Jerolmack, 2009). This is being linked to unsteady discontinuous sedimentation. As such, the observed increase in sediment deposition cannot only be explained by a true increase due to variations in driving forces, but also by an apparent increase caused by such scaling effects. As there is no systematic sampling for shallower or deeper Holocene deposits, sampling density (in depth) can be more or less equal for the entire Holocene sequence. As such, higher sedimentation rates for shorter time spans are a logical consequence. Lower sedimentation rates, and thus more or longer periods with little or no sedimentation, are also an essential part the sediment dynamics. In order to correct for a possible measuring period dependence in sedimentation rates, dating should be performed homogeneously in time over the Holocene period, which implies for most dated places in the Dijle catchment that the sampling density in depth should largely vary. A coupling between the calculated sedimentation rates or (relative) mass accumulation rates and the fluvial architecture and site-specific sedimentation histories also indicates that time dependency is not the only explaining factor for high recent rates.

Table 4. Model efficiencies (ME) for the different scenarios for relative mass accumulation rates compared to calculated relative mass accumulation rates based on radiocarbon ages of the Dijle catchment.

Scenario: increase from	ME colluvial dates	ME alluvial dates	ME alluvial dates excluding Bonlez U
2000 BC	0.46	−0.48	−0.36
1000 BC	0.73	−0.23	−0.09
1 AD	0.72	−0.04	0.09
500 AD	0.56	−0.05	0.05
1000 AD	0.03	−0.19	−0.13

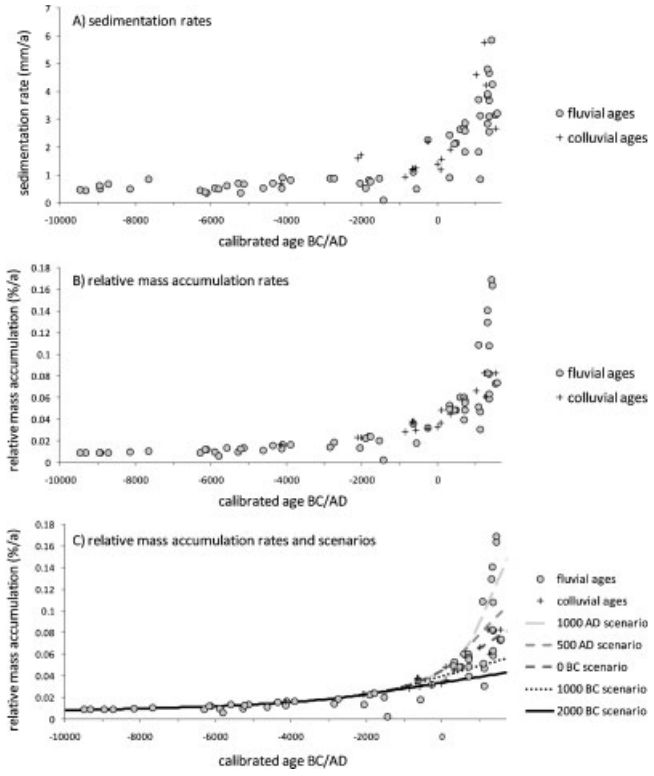

Figure 8. Sedimentation rates (SR) and relative mass accumulation rates (MR) plotted vs. depth for the available radiocarbon dates in the Dijle catchment. (A) Sedimentation rates; (B) relative mass accumulation rates; (C) relative mass accumulation rates including the different modelled scenarios.

Cumulative probability functions of radiocarbon ages

The CPD of floodplain fines ages (Fig. 9A) shows peaks around 1500–1300 BC, 250–750 AD and 1250–1650 AD. The CPD of colluvial ages (Fig. 9B) shows peaks around 4300–4000 BC, 2250–1900 BC, 900 BC–500 AD, 900 AD–1400 AD and 1450 AD to present. The charcoal ages from Bilande are considered to be reworked and redeposited, and therefore they were not included in the original analysis. However, they also indicate phases of past colluviation more upstream, which was subsequently eroded (Lang and Hönscheidt, 1999), and therefore they can also be introduced into the CPD (Fig. 9C). The resulting CPD differs slightly: there are additional peaks between 2000 and 1000 BC. All these CPDs rely on a low number of ages which cause a high sensibility to individual samples. The combined CPD for aggradation ages (Fig. 10, B and C) shows comparable peaks, with aggradation ages concentrated after 2000 BC with lower probabilities at ca. 1900 BC, ca. 1650 BC, 1100–900 BC, ca. 800 BC, ca. 400 BC and 1400–1450 AD.

The CPD off all peat ages (Fig. 10A) shows peaks at 9650–9300 BC, 9150–8650 BC, 8250 BC, 7750–7600 BC, 6350–5750 BC, 5600–5000 BC, 4700–4550 BC, 4450–3800 BC, 2850–2550 BC, 2150–1450 BC, 750–50 BC, 220–400 AD, 650–800 AD and 1000–1500 AD. Compared with the aggradation ages, the stability ages show a larger scatter.

Although the CPDs in this study are based on low numbers of data, which biases their interpretation, we consider that they still provide a framework for an objective analysis of the available radiocarbon ages. From the CPDs it is clear that aggradation, both colluvial and alluvial, occurred mainly during the end of the Holocene, after 2000 BC. The given data

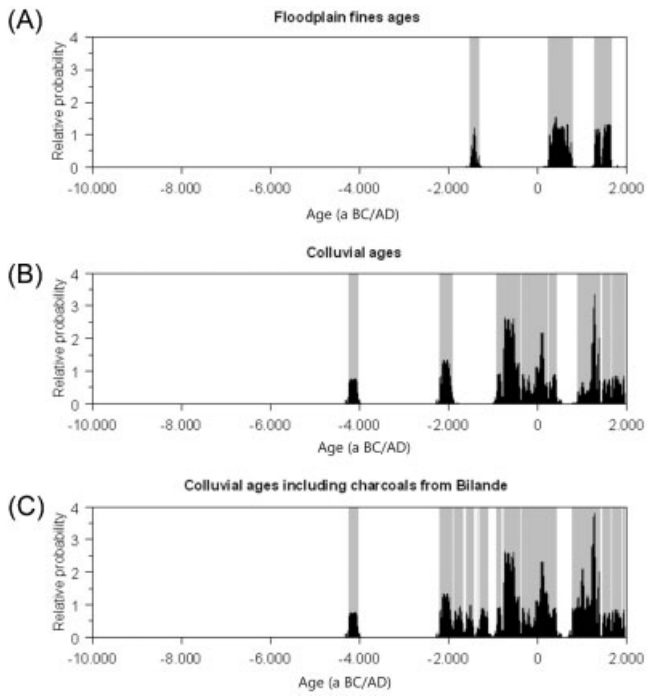

Figure 9. Cumulative probability functions (CPDs) for radiocarbon ages in the Dijle catchment. Probabilities are divided by the probability of equally spaced ages. The grey shaded area indicates where the relative probability is larger than average. (A) Floodplain fines ($n = 10$); (B) colluvial deposits ($n = 21$); (C) colluvial deposits including rejected charcoal ages from Bilande ($n = 29$).

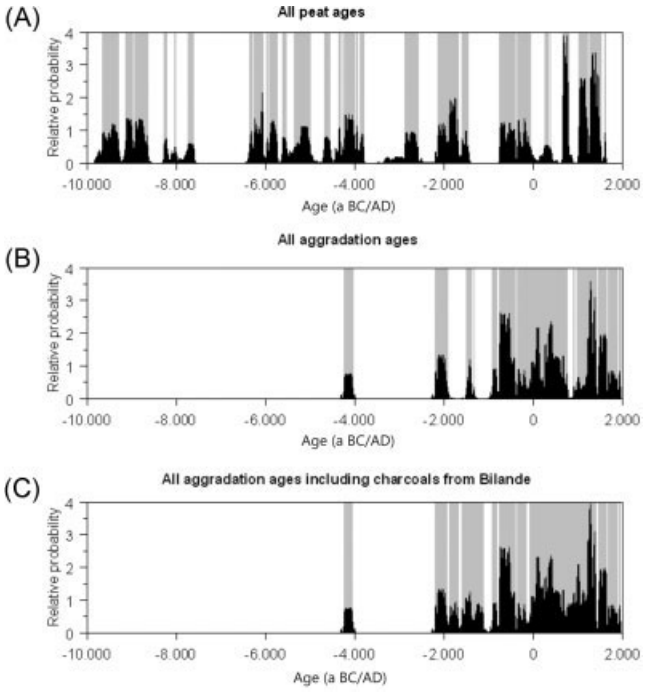

Figure 10. Cumulative probability functions (CPDs) for radiocarbon ages in the Dijle catchment. Probabilities are divided by the probability of equally spaced ages. The grey shaded area indicates where the relative probability is larger than average. (A) All peat ages ($n = 49$); (B) all aggradation ages ($n = 31$); (C) all aggradation ages including rejected charcoal ages from Bilande ($n = 39$).

suggest that between 2000 BC and 1 AD colluvial aggradation was more important than alluvial aggradation. Peat ages, indicating stable phases, are rather well spread over the Holocene. The simultaneous occurrence of stability and aggradation peaks during the last 4 ka suggests a spatial heterogeneity within the catchment: while some parts are prone to aggradation, floodplains in other parts are stable. Such a spatial heterogeneity can point to different responses of floodplains to the same external forcings, or to heterogeneity in these external forcings.

Time-differentiated sediment budget

Table 5 and Fig. 11 show the results of the temporal differentiated sediment budget for the two scenarios described above. These results are based on the dating results and thus show comparable patterns of varying sedimentation rates. As colluvial valley deposition is very low for the first period (early Holocene to 2000 BC), scenario 1 yields a hillslope sediment delivery ratio (HSDR) for this first period of 96%, which is very high. These HSDR rates are considered unrealistically high by Verstraeten *et al.* (2009a). Using scenario 2, HSDR drops to 83%, which is at first sight a more realistic value. On the other hand, hillslope colluvial deposition is often reported to be associated with agricultural practices and the creation of lynchets (e.g. Houben, 2006, 2008). Colluvial deposition is also very rare or absent in the historical forests of the catchment, for which we can assume that these experienced only a minimal anthropogenic impact (e.g. Langohr and Sanders, 1985). Indeed, before 4000 BC no traces of colluvial deposition could be found so far in the Dijle catchment (see CPD analysis), which would mean that the HSDR is indeed near 100%. Off course, the spatial representativeness of our dataset is limited and it cannot therefore be excluded that some slopes do have limited colluvial deposits. Based on all these observations both scenario 1 and 2 can be valid (Fig. 12).

Table 5. Temporal differentiated sediment budget for the Dijle catchment, using two different scenarios (see text).

	Hillslope erosion (Tg)	Hillslope deposition (Tg)	Colluvial valley deposition (Tg)	Hillslope export (Tg)	HSDR (%)	Tributary floodplain deposition (Tg)	Trunk valley floodplain deposition (Tg)	Export (Tg)	SDR (%)
Scenario 1									
Period 1: 9000 BC–2000 BC	69.2	1.0	1.8	66.4	95.9	32.0	13.8	20.5	29.7
Period 2: 2000 BC–1000 AD	209.3	42.6	73.8	93.0	44.4	26.8	26.6	39.5	18.9
Period 3: 1000 AD–present	535.4	75.9	131.5	328.1	61.3	132.6	78.6	116.8	21.8
Scenario 2									
Period 1: 9000 BC–2000 BC	79.9	11.7	1.8	66.4	83.1	32.0	13.8	20.5	25.7
Period 2: 2000 BC–1000 AD	195.4	28.7	73.8	93.0	47.6	26.8	26.6	39.5	20.2
Period 3: 1000 AD–present	538.6	79.1	131.5	328.1	60.9	132.6	78.6	116.8	21.7
Total Holocene	814.0	119.5	207.1	487.4	59.9	191.5	119.1	176.9	21.7

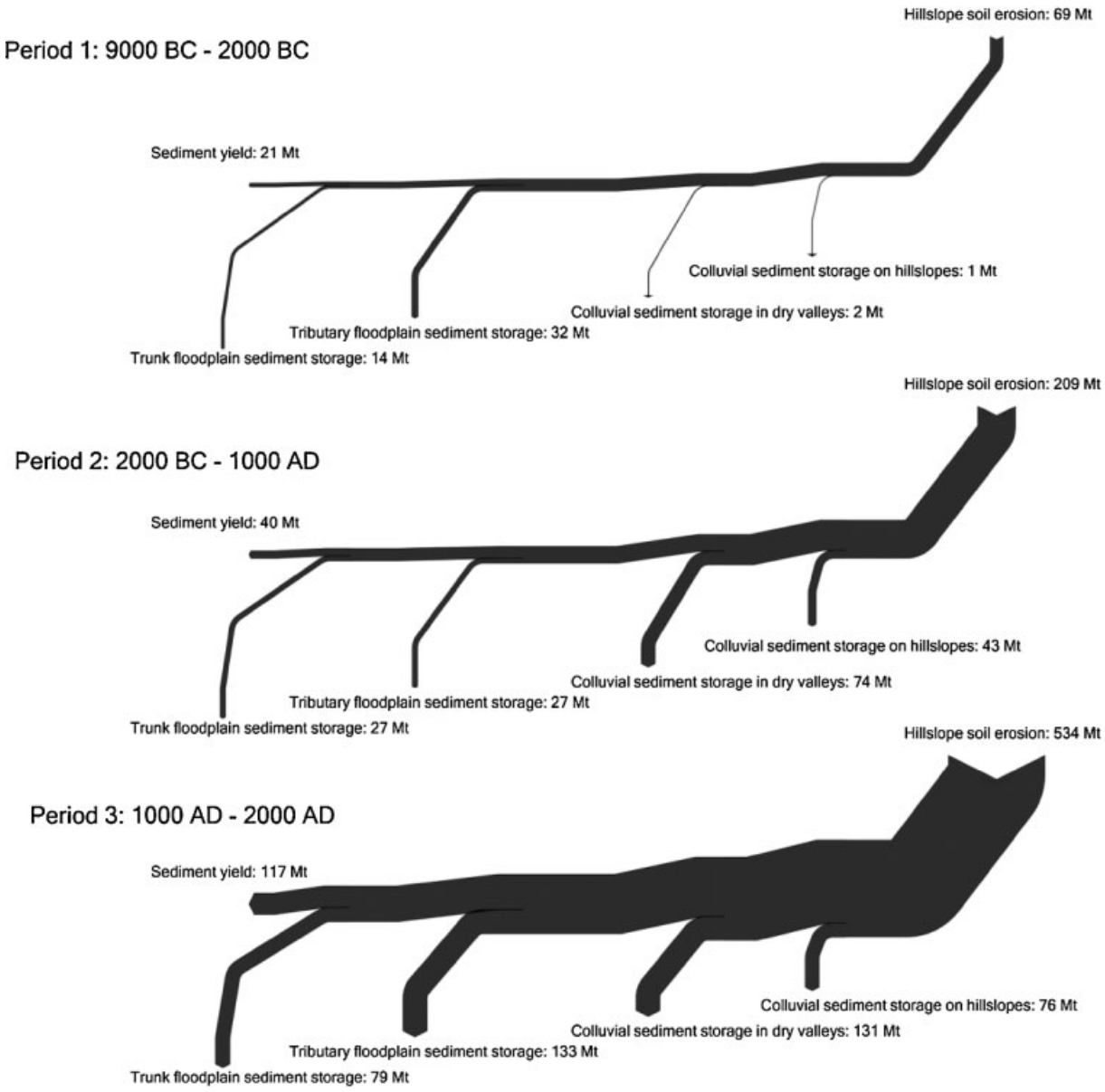

Figure 11. Time-differentiated sediment budget for the Dijle catchment, using scenario 1 for the time differentiation of the soil erosion masses.

The results (Fig. 12) show that during the second period (2000 BC–1000 AD) colluvial deposition is more important than alluvial deposition. The relative importance of floodplain deposition increases again during the last period (1000 AD–present). This demonstrates a lag time between colluvial storage and floodplain storage, as was demonstrated before.

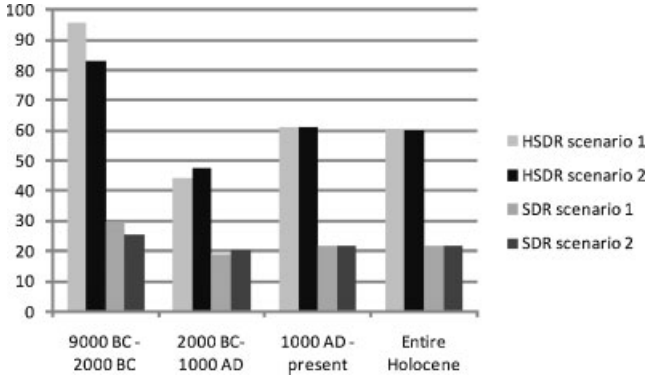

Figure 12. Evolution of SDR and HSDR in the Dijle catchment, using the two scenarios to construct the time-differentiated sediment budget.

Discussion

Several methods were used to analyse the available radiocarbon dates (Table 6). Relative sedimentation and mass accumulation rates were constructed for each individual coring site and a general pattern was extracted (Fig. 8). Construction of these diagrams, especially the mass accumulation, requires the availability of a detailed coring description (e.g. layer thickness, texture, OM and DBD). Owing to the low number of dates per coring site the interpretation suffers from a large averaging effect and a low spatial resolution. The older the sample, the larger this averaging effect will be, causing a lower temporal resolution and a decreased sensitivity (Hoffmann *et al.*, 2009). Therefore only long-term changes in sedimentation rates can be identified. On the other hand, this method allows the reconstruction of site-specific sedimentation histories. Local deviations from the general pattern can give more insight into the spatial variability of the catchment sediment dynamics. Scenarios of deposition rates can be developed and compared with the distribution of the ages to come to general conclusions about sedimentation history.

Compared to the sedimentation rate analysis of the Rhine catchment (Hoffmann *et al.*, 2009), the methodology was

Table 6. Overview of the different methods used for the analysis of radiocarbon ages and the derived sedimentation history of the Dijle catchment: output parameter, temporal resolution, derived start of the increase in colluvial sedimentation and derived start of the increase in alluvial sedimentation. Temporal resolutions are partially based on Hoffmann *et al.* (2009).

	Sedimentation history per site	Mass accumulation rate	Frequency distribution
Output parameter	(Relative) sedimentation rate	(Relative) sedimentation rates	Probability densities of radiocarbon ages
Temporal resolution	Variable, 100–5000 a	Variable, decreasing with age	50–200 a
Start of increasing colluvial sedimentation	First increase 4160–600 BC Main deposition last 1000 a	1000 BC	4300 BC
Start of increasing alluvial sedimentation	First increase 4000–500 BC Second increase ~1000 AD	1 AD	1500 BC

improved in three ways. This improved analysis was facilitated by the availability of a detailed coring description which was missing in the synthetic analysis of Hoffmann *et al.* (2009). By using relative mass accumulation rates instead of volumetric sedimentation rates, the calculated values take into account the large variations in organic material of floodplain sediments. Peat layers can be responsible for an important vertical aggradation of the floodplain, especially during the early Holocene, which does not correspond to important sediment accumulation due to the low mineral content of these layers. Additionally, the use of relative rates excludes the effect of local differences in total Holocene accumulation. Finally, the use of relative rates and the methodology used for the models results in equal total Holocene sediment accumulation amounts for all models (100%), whereas Hoffmann *et al.* (2009) use models which yield different total Holocene accumulation amounts (in total thickness of the Holocene deposit). As a result, our models allow a more straightforward comparison with the calculated rates.

The construction of CPDs based on radiocarbon ages provides a detailed image of phases during which the different processes were active. CPDs were constructed for several groups of radiocarbon data, representing stability or aggradation of the floodplain (see also Hoffmann *et al.*, 2009; Macklin *et al.*, 2010). Interpretation of these CPDs suffers largely from the limited amount of available radiocarbon dates: peaks can be caused by a single radiocarbon date, which makes this method extremely sensitive for outliers. Spatial heterogeneity of processes can also play a role: while stability dominates in one part of the catchment, aggradation can dominate elsewhere. The CPD method can provide insight into short time variations (Hoffmann *et al.*, 2009) and is thus more suited to studying the effects of short time variations of the driving forces. Additionally there are two major methodological drawbacks (Hoffmann *et al.*, 2009). First, the probability frequencies cannot be transferred into volumes or fluxes. Where the CPD of aggradation ages shows comparable or even more dominant peaks for the period around 1000 BC compared to those for the period after 1000 AD, the other applied methods suggest that the fluxes for the last period are more important. Second, low probabilities do not necessarily suggest low activities but rather a lack of dating evidence, which can be caused by a low preservation potential or by the sampling method. Indeed, the CPD of the peat ages shows no peaks between 8000 and 6000 BC, which is caused by the sampling strategy: often only the top and the base of the basal peat layer are sampled and nothing in between, and as a result few dates are available for the middle of the period with peat formation. An increased number of available ages would improve the application of this method in the Dijle catchment. It remains unclear, however, how many dates are needed to construct CPDs (Hoffmann *et al.*, 2008).

Comparison of CPDs of the Dijle catchment with those from other European catchments is biased by the differences in methodology used, the related different objectives and the limited number of ages available in this study. For Poland the database was divided into different groups, excluding a group representing the overbank deposition (Starkel *et al.*, 2006). Conclusions are mainly based on ages of channel facies and abundance of palaeochannels. Dates coinciding with overbank aggradation above peat layers peak mainly in the expansion period of agriculture during the late Roman period and the 11–15th centuries AD (Starkel *et al.*, 2006). For Great Britain, phases of major flooding are identified based on a database of radiocarbon ages (Macklin and Lewin, 2003). Lewin *et al.* (2005) classify the dates into groups, including a group representing dated floodplain surfaces (overbank) ages. The results show that floodplain sedimentation peaks mainly during the later Holocene and alluviation rates were not started but enhanced by anthropogenic effects. The greater availability of fine-grained material by weathering, with the progressing Holocene, can also play a role. Further, also the importance of preservation potential is stressed. For Great Britain, Macklin *et al.* (2010) have recently reviewed the CPDs for different depositional environments. Comparable to the results of this study, an acceleration in overbank floodplain sedimentation is reported after 1 cal ka BP, for the first time recognising an unequivocal anthropogenic signal affecting the British rivers. In this study we used an approach comparable with the approach used in Germany (Hoffmann *et al.*, 2008) and for the Rhine catchment (Hoffmann *et al.*, 2009). Due to the size of the database we used in our study, fewer groups could be differentiated. For the Rhine catchment (Hoffmann *et al.*, 2009), stable floodplain environments occurred during the early and Middle Holocene (9000–5000 BC), followed by increased floodplain deposition in the Late Holocene (since 1500 BC). Within the last period, peaks of higher probabilities for floodplain deposition are reported at 1000 BC, 300 BC and 1100 AD, while lower probabilities occur at 700 BC, 200 AD and 1400 AD. Colluvial ages do not show a general trend in this catchment, but most important peaks of increased probabilities are observed around 7000 BC, 5500 BC, 2500 BC and since 1200 AD. The database for the whole of Germany (Hoffmann *et al.*, 2008) overlaps largely with the database from the Rhine catchment (Hoffmann *et al.*, 2009), resulting in the same patterns.

In this study a large number of dated cross-sections and dates were used to provide a catchment-wide overview of the sedimentation history. By using a large number of cross-sections and corings, the influence of local variations is minimised. When considering site-specific sedimentation rates (Fig. 6) the variation is relatively high. Comparison of the relative accumulated mass of the Bonlez U and Bonlez D cross-

sections indicates that there are important differences between both cross-sections, although cross-section Bonlez U is located only 2.0 km upstream of Bonlez D. As no major tributaries join the Train valley between the study sites, the upstream catchment of both sites is only slightly different. These observations stress the importance of using dating results from different sites to obtain insight into the catchment sediment dynamics. Local sedimentation histories will be influenced by environmental variations in the upstream catchment of the studied site, and even with an almost identical upstream catchment individual coring sites can show a different sedimentation history. As a result, simple extrapolation of local sedimentation histories to a larger catchment is not justified.

The different methods used to evaluate the radiocarbon dates of the Dijle catchment yield comparable sedimentation histories. Evidence for early Holocene colluvial deposition is lacking and first colluvial deposition is reported from ca. 4000 BC on, coinciding with the Neolithic Period. Colluviation appears to become more important between 2000 BC and 500 BC, and a second increase occurs between 0 AD and 1300 AD. The age/depth and frequency distribution analysis of radiocarbon dates suggest that the increase in alluvial deposition occurs later than the increase in colluvial deposition. For most sites the increase in floodplain deposition starts somewhere between 4000 and 500 BC, while the major part of floodplain sedimentation occurred since ca. 1000 AD. This general pattern of colluvial and alluvial deposition coincides with the general pattern of an increasing intensity in agricultural activities from the Neolithic Period on. Little evidence exists for the influence of climatic variations. When studying the sedimentation rates at the Bilande site in detail, the main sedimentation phase occurred somewhere between 1150 and 1450 AD. In other catchments sedimentation phases during the high Middle Ages are linked to a wetter climate during the 14th century and especially due to major rainfall events in 1342 AD (e.g. Bork *et al.*, 1998), while the same period coincides with a peak in agricultural activities (e.g. Bork *et al.*, 1998). It is unclear from the available data whether the peak in sediment deposition is caused by increased agricultural pressure, a wetter climatic phase or a combination of both.

An apparent lag time is reported between the increase in colluvial and alluvial deposition, which can be created by a lag time between catchment disturbance and its influence on the floodplain deposition, or by a threshold which has to be met before a disturbance influences floodplain deposition. Given observations in other catchments (e.g. sediment cascade model; Lang and Hönscheidt, 1999) and the earlier increase in colluvial deposition compared to alluvial deposition, we hypothesise that it is rather a threshold that has to be met than a lag time between erosion and sedimentation.

An apparent lag time or threshold between changes in catchment environment and changes in deposition rates is evident for other catchments (e.g. Kalicki *et al.*, 2008; Lespez *et al.*, 2008; Trimble, 2009). Comparable to the Dijle catchment, the sediment budget of Coon Creek, Wisconsin, also shows a downstream shift of the sediment dynamics following catchment disturbances (Trimble, 1983, 1999, 2009). Increase of sediment erosion caused a downstream shifting wave of sediment deposition, while decrease of sediment erosion caused a downstream shifting evolution of cessation of floodplain accumulation or even floodplain erosion.

An important limitation on the temporal differentiated sediment budget is, however, that it does not take into account the repeated reworking and redeposition of sediments. Several periods of deposition and erosion of colluvial deposits have possibly occurred, as demonstrated, for example, by Lang and Hönscheidt (1999) and supported by the presence of reworked charcoals in the colluvial deposits at Bilande. There is no field evidence to quantify the importance of the reworking of sediments. Reworking can have an important influence on the sediment budget: due to a lower preservation potential (e.g. Lewin and Macklin, 2003) the older colluvial deposits are possibly underestimated compared to more recent deposits. Therefore the total erosion and deposition amounts will be underestimated, also resulting in errors in the sediment delivery ratio (SDR) and HSDR. The absence of large amounts of colluvial material in the historical forests of the catchment (see above) suggests, however, that reworking of colluvial deposits since the early Middle Ages of older material will be limited. Additional budgeting of old colluvial deposits in these historical forest could supply more information on the importance of reworking in sediment budgeting. A main advantage of the time-differentiated sediment budget is that it provides an integrated sediment dynamics history of the catchment. The site-specific sedimentation histories demonstrate that there is a large variation in sedimentation history between sites. Therefore a lumped approach is preferable, integrating the sedimentation history over space and time. The resulting averaged trend can be displayed with a larger confidence. A main advantage of using a time-differentiated sediment budget over site-specific sedimentation curves (Figs. 5–7) or analysis of the radiocarbon dates database (Figs. 8–10) is that it allows the quantification of the changing importance of different sinks and links in the sediment budget. Although MR calculations and site-specific sedimentation histories allow a quantification of processes, the analysis remains qualitative and a quantification of fluxes is not possible. By using a spatial and temporal integrated approach, the results are filtered for variability in the different processes, providing a catchment-wide pattern and enabling a more robust correlation with the environmental changes, for which information is often also available on a catchment scale. By quantifying the different processes and links, variations in connectivity between the different components of the sediment dynamics can be quantified.

The different methodologies applied in this work indicate an important influence of anthropogenic land use changes on floodplain sedimentation in the Dijle catchment. However, the dating resolution does not allow identifying the influence of short-term climatic variations, lasting some decades or even a few centuries, on the catchment processes. A more detailed temporal framework is needed to identify such phases. An extension of the radiocarbon database could possibly address this problem, as the identification of shorter phases becomes more reliable, depending on fewer data points (e.g. Macklin *et al.*, 2010). Different studies have indicated the importance of climatic events on catchment and fluvial processes (e.g. Macklin and Lewin, 2003; Starkel *et al.*, 2006). Land use changes may have made the landscape more sensitive to climatic events (see, for example, Knox, 2001), and we hypothesise that probably the interplay between land use changes and climatic events has determined the Holocene sediment dynamics of the Dijle catchment.

Conclusions

In this study, AMS radiocarbon and OSL dating were applied to the dating of alluvial and colluvial sediments in the medium-sized Dijle catchment. A database of 81 radiocarbon data values was developed and from this sedimentation rates and cumulative frequency distributions were analysed.

The results for the Dijle catchment show that there is a large variation in sedimentation history between the different study sites and that data from a single coring cannot simply be extrapolated to an entire catchment. Dating different sites within the same catchment can provide deeper insight into catchment-

wide processes. In addition, the construction of sedimentation rates and relative mass accumulation rates allows a catchment-wide insight into the sedimentation history. Comparably, the use of cumulative probability functions of radiocarbon ages provides an important methodological tool for the analysis of catchment-wide floodplain or colluvial aggradation and stability phases.

Results show that net floodplain aggradation in the studied catchment is much higher in recent periods then before. The detailed sedimentation history shows the influence of anthropogenic land use on both colluvial and alluvial aggradation since Neolithic times. Changes in sediment dynamics for Neolithic times and possibly also for subsequent periods was limited, and more important changes occurred only later, with the most important sedimentation phase during the last 1 ka. An influence of climatic variation on the studied sedimentary archives could not be identified, which can be attributed to the absence of such an influence or to the dating resolution, which does not allow the detection of short duration variations. Possibly land use changes have made the catchment more sensitive to climatic events (e.g. Knox, 2001), and the interplay between both land use changes and climatic events may have determined the catchment sediment dynamics during the Holocene. A further refinement of the dating resolution or a modelling study is necessary to validate this hypothesis. The results also indicate the large variability between the different studied cores, even when they are located in the same fluvial system at a short distance. This stresses the importance of studying several profiles in order to incorporate local variations and in order to develop a catchment-wide sedimentation pattern.

The time-differentiated sediment budget of the Dijle catchment indicates that there are important variations in the relative importance of colluvial and alluvial deposition as sediment sinks. We hypothesised that the resulting lag time between colluvial and alluvial sedimentation can be attributed to a threshold that has to be met in soil erosion and/or sediment transport in order to result in certain amounts of floodplain deposition. This time lag indicates the importance of internal system dynamics. Studies concerning entire catchment and sediment pathways, like sediment budget studies, can help in understanding the temporal and spatial dynamics of the sediments within those catchments (e.g. Verstraeten *et al.*, 2009a). Modelling studies can also provide an important contribution to the understanding of past sediment dynamics, as such models would allow control of the variations of each driving force (e.g. Ward *et al.*, 2009).

Acknowledgements. This research is part of a project funded by the Research Foundation Flanders (FWO, research project G.0583.06), and by the Interuniversity Attraction Poles Programme—Belgian State–Belgian Science Policy, project P6/22. Their support is gratefully acknowledged. The authors would also like to thank Bjorn Dieu, Jeroen Monsieur, and the several MSc and PhD students in physical geography for their assistance during fieldwork. We would also like to thank M. Macklin and T. Hoffmann for reviewing this paper and providing useful comments.

Abbreviations. AMS, accelarator mass spectrometry; a.s.l., above sea level; BLSL, blue light stimulated luminescence; CPD, cumulative probability distribution; HSDR, hillslope sediment delivery ratio; IRSL, infrared stimulated luminescence; ME, model efficiency; MR, relative mass accumulation rate; OSL, optically stimulated luminescence; SDR, sediment delivery ratio; SR, sedimentation rate.

References

Adamiec G, Aitken MJ. 1998. Dose-rate conversion factors: update. *Ancient TL* **16**: 37–50.

Aitkin MJ. 1985. *Thermoluminescence Dating*. Academic Press, London.

Beach T. 1994. The fate of eroded soil: sediment sinks and sediment budgets of agrarian landscapes in southern Minnesota, 1851- 1988. *Annals of the Association of American Geographers* **84**: 5–28.

Bisutti I, Hilke I, Raessler M. 2004. Determination of total organic carbon: an overview of current methods. *Trends in Analytical Chemistry* **23**: 716–726.

Bork H-R, Bork H, Dalchow C, *et al*. 1998. *Landschaftsentwicklung in Mitteleuropa: Wirkungen des Menschen auf Landschaften*. Klett-Perthes: Gotha, Germany.

Bøtter-Jensen L, Andersen CE, Duller GAT, Murray AS. 2003. Developments in radiation, stimulation and observation facilities in luminescence measurements. *Radiation Measurements* **37**: 535–541.

Bronk Ramsey C. 2001. Development of the radiocarbon calibration program OxCal. *Radiocarbon* **43**: 355–363.

Bronk Ramsey C. 2009. Bayesian analysis of radiocarbon dates. *Radiocarbon* **51**: 337–360.

Chiverrell RC, Foster GC, Thomas GSP, *et al*. 2009. Robust chronologies for landform development. *Earth Surface Processes and Landforms* **34**: 319–328.

de Moor J, Verstraeten G. 2008. Alluvial and colluvial sediment storage in the Geul River catchment (The Netherlands): combining field and modelling data to construct a Late Holocene sediment budget. *Geomorphology* **95**: 487–503.

De Smedt P. 1973. Paleogeografie en kwartair-geologie van het confluentiegebied Dijle-Demer. *Acta Geographica Lovaniensia* **11**: 141 pp.

Dotterweich M. 2008. The history of soil erosion and fluvial deposits in small catchments of central Europe: deciphering the long-term interaction between humans and the environment – a review. *Geomorphology* **101**: 192–208.

Duller GAT. 2003. Distinguishing quartz and feldspar in single grain luminescence measurements. *Radiation Measurements* **37**: 161–165.

Foulds S, Macklin M. 2006. Holocene land-use change and its impact on river basin dynamics in Great Britain and Ireland. *Progress in Physical Geography* **30**: 589–604.

Fryirs K, Brierley GJ. 2001. Variability in sediment delivery and storage along river courses in Bega catchment, NSW, Australia: implications for geomorphic river recovery. *Geomorphology* **38**: 237–265.

Fuchs M, Lang A. 2001. OSL dating of coarse-grain fluvial quartz using single-aliquot protocols on sediments from NE Peloponnese, Greece. *Quaternary Science Reviews* **20**: 783–787.

Hoffmann T, Erkens G, Cohen KM, *et al*. 2007. Holocene floodplain sediment storage and hillslope erosion within the Rhine catchment. *Holocene* **17**: 105–118.

Hoffmann T, Lang A, Dikau R. 2008. Holocene river activity: analysing ^{14}C-dated fluvial and colluvial sediments from Germany. *Quaternary Science Reviews* **27**: 2031–2040.

Hoffmann T, Erkens G, Gerlach R, *et al*. 2009. Trends and controls of Holocene floodplain sedimentation in the Rhine catchment. *Catena* **77**: 96–106.

Houben P. 2006. A Holocene sediment budget for the Rockenberg catchment. Pre-workshop field guide. In *Open Lucifs Workshop*, 2006.

Houben P. 2008. Scale linkage and contingency effects of field-scale and hillslope-scale controls of long-term soil erosion: anthropogeomorphic sediment flux in agricultural loess watersheds of Southern Germany. *Geomorphology* **101**: 172–191.

Kalicki T, Sauchyk S, Calderoni G, *et al*. 2008. Climatic versus human impact on the Holocene sedimentation in river valleys of different order: examples from the upper Dnieper basin, Belarus. *Quaternary International* **189**: 91–105.

Knox JC. 2001. Agricultural influence on landscape sensitivity in the Upper Mississippi River Valley. *Catena* **42**: 193–224.

Knox JC. 2006. Floodplain sedimentation in the Upper Mississippi Valley: natural versus human accelerated. *Geomorphology* **79**: 286–310.

Lang A. 2008. Recent advances in dating and source tracing of fluvial deposits. In *Sediment Dynamics in Changing Environments*, Schmidt J, Cochrane T, Phillips C, *et al*. Publication 325. IAHS: Wallingford, Oxon, UK; 3–12.

Lang A, Hönscheidt S. 1999. Age and source of colluvial sediments at Vaihingen-Enz, Germany. *Catena* **38**: 89–107.

Langohr R, Sanders J. 1985. The Belgian Loess Belt in the last 20 000 years: evolution of soils and relief in the Zonien Forest. In *Soils and Quaternary Landscape Evolution*, Boardman J editor. Wiley: Chichester; 359–371.

Lespez L, Clet-Pellerin M, Limondin-Lozouet N, *et al*. 2008. Fluvial system evolution and environmental changes during the Holocene in the Mue valley (Western France). *Geomorphology* **98**: 55–70.

Lewin J, Macklin M. 2003. Preservation potential for Late Quaternary river alluvium. *Journal of Quaternary Science* **18**: 107–120.

Lewin J, Macklin M, Johnstone E. 2005. Interpreting alluvial archives: sedimentological factors in the British Holocene fluvial record. *Quaternary Science Reviews* **24**: 1873–1889.

Macklin MG, Lewin J. 2003. River sediments, great floods and centennial-scale Holocene climate change. *Journal of Quaternary Science* **18**: 101–105.

Macklin M, Benito G, Gregory K, *et al*. 2006. Past hydrological events reflected in the Holocene fluvial record of Europe. *Catena* **66**: 145–154.

Macklin M, Jones A, Lewin J. 2010. River response to rapid Holocene environmental change: evidence and explanation in British catchments. *Quaternary Science Reviews* **29**: 1555–1576.

Messerli B, Grosjean M, Hofer T, *et al*. 2000. From nature-dominated to human-dominated environmental changes. *Quaternary Science Reviews* **19**: 459–479.

Meybeck M. 2003. Global analysis of river systems: from Earth system controls to Anthropogene syndromes. *Philosophical Transactions of the Royal Society of London, Series V* **358**: 1935–1955.

Mullenders W, Gullentops F, Lorent J, *et al*. 1966. Le Remblement de la vallée de la Nethen. *Acta Geographica Lovaniensia* **4**: 169–181.

Murray AS, Wintle AG. 2000. Luminescence dating of quartz using an improved single-aliquot regenerative-dose protocol. *Radiation Measurements* **32**: 57–73.

Murray AS, Wintle AG. 2003. The single aliquot regenerative dose protocol: potential for improvements in reliability. *Radiation Measurements* **37**: 377–381.

Nash JE, Sutcliffe JV. 1970. River flow forecasting through conceptual models, a discussion of principles. *Journal of Hydrology* **10**: 282–290.

Notebaert B. 2009. *Sensitivity of river systems to human actions and climatic events across different environments: a Holocene perspective*. PhD thesis. Department Earth and Environmental Sciences, KU Leuven, Belgium.

Notebaert B, Verstraeten G, Rommens T, *et al*. 2009. Establishing a Holocene sediment budget for the river Dijle. *Catena* **77**: 150–163.

Page MJ, Trustrum NA, Dymond JR. 1994. Sediment budget to assess the geomorphic effect of a cyclonic storm, New Zealand. *Geomorphology* **9**: 169–188.

Prescott JR, Hutton JT., 1994. Cosmic ray contributions to dose rates for luminescence and ESR dating: large depths and long-term time variations. *Radiation Measurements* **23**: 497–500.

Reid L, Dunne T. 2003. Sediment budgets as an organizing framework in fluvial geomorphology. In *Tools in Fluvial Geomorphology*, Kondolf M, Piégay H editors. Wiley: New York; 463–500.

Reimer PJ, Baillie MGL, Bard E, *et al*. 2004. IntCal04 Terrestrial radiocarbon age calibration,0-26 ka BP. *Radiocarbon* **46**: 1029–1058.

Rommens T. 2006. *Holocene sediment dynamics in a small river catchment in central Belgium*. PhD thesis. Department Geography–Geology, KU Leuven, Belgium.

Rommens T, Verstraeten G, Bogman P, *et al*. 2006. Holocene alluvial sediment storage in a small river catchment in the loess area of central Belgium. *Geomorphology* **77**: 187–201.

Rommens T, Verstraeten G, Peeters I, *et al*. 2007. Reconstruction of late-Holocene slope and dry valley sediment dynamics in a Belgian loess environment. *Holocene* **17**: 777–788.

Sadler PM. 1981. Sediment accumulation rates and the completeness of stratigraphic sections. *Journal of Geology* **89**: 569–584.

Schumer R, Jerolmack DJ. 2009. Real and apparent changes in sediment deposition rates through time. *Journal of Geophysical research – Earth Surface* **114**: 12 pp. [F00A06].

Slaymaker O. 2003. The sediment budget as conceptual framework and management tool. *Hydrobiologia* **494**: 71–82.

Starkel L, Soja R, Michczynska DJ. 2006. Past hydrological events reflected in the Holocene history of Polish rivers. *Catena* **66**: 24–33.

Thorndycraft V, Benito G. 2006a. Late Holocene fluvial chronology of Spain: the role of climatic variability and human impact. *Catena* **66**: 34–41.

Thorndycraft V, Benito G. 2006b. The Holocene fluvial chronology of Spain: evidence from a newly compiled radiocarbon database. *Quaternary Science Reviews* **25**: 223–234.

Törnqvist T, Dejong A, Oosterbaan W, *et al*. 1992. Accurate dating of organic deposits by AMS ^{14}C measurement of macrofossils. *Radiocarbon* **34**: 566–577.

Trimble SW. 1983. A sediment budget for Coon Creek basin in the Driftless Area, Wisconsin, 1853- 1977. *American Journal of Science* **283**: 454–474.

Trimble SW. 1999. Decreased rates of alluvial sediment storage in the Coon Creek Basin, Wisconsin, 1975-93. *Science* **285**: 1244–1246.

Trimble SW. 2009. Fluvial processes, morphology and sediment budgets in the Coon Creek Basin, WI, USA, 1975- 1993. *Geomorphology* **108**: 8–23.

Vandenberghe D. 2004. *Investigation of the optically stimulated luminescence dating method for application to young geological sediments*. PhD thesis, Universiteit Gent, Belgium.

Vandenberghe D, De Corte F, Buylaert J-P, *et al*. 2008. On the internal radioactivity in quartz. *Radiation Measurements* **42**: 771–775.

Verstraeten G, Poesen J. 2001. Factors controlling sediment yield from small intensively cultivated catchments in a temperate humid climate. *Geomorphology* **40**: 123–144.

Verstraeten G, Rommens T, Peeters I, *et al*. 2009a. A temporarily changing Holocene sediment budget for a loess-covered catchment (central Belgium). *Geomorphology* **108**: 24–34.

Verstraeten G, Lang A, Houben P. 2009b. Human impact on sediment dynamics: quantification and timing. *Catena* **77**: 77–80.

Walling D, Quine T. 1993. Using Chernobyl-derived fallout radionuclides to investigate the role of downstream conveyance losses in the suspended sediment budget of the river Severn, United Kingdom. *Physical Geography* **14**: 239–253.

Walling DE, Russel M, Hodgkinson R, *et al*. 2002. Establishing sediment budgets for two small lowland agricultural catchments in the UK. *Catena* **47**: 323–353.

Walling DE, Collins A, Jones P, *et al*. 2006. Establishing fine-grained sediment budgets for the Pang and Lambourn LOCAR catchments, UK. *Journal of Hydrology* **33**: 126–141.

Ward P, van Balen R, Verstraeten G, *et al*. 2009. The impact of land use and climate change on late Holocene and future suspended sediment yield of the Meuse catchment. *Geomorphology* **103**: 389–400.